Real-time Measurement System for Evaluation of the Carotid Intima-Media Thickness With a Robust Edge Operator

Francesco Faita, PhD, Vincenzo Gemignani, PhD, Elisabetta Bianchini, PhD, Chiara Giannarelli, MD, PhD, Lorenzo Ghiadoni, MD, PhD, Marcello Demi, PhD

Objective. The purpose of this report is to describe an automatic real-time system for evaluation of the carotid intima-media thickness (CIMT) characterized by 3 main features: minimal interobserver and intraobserver variability, real-time capabilities, and great robustness against noise. ***Methods.*** One hundred fifty carotid B-mode ultrasound images were used to validate the system. Two skilled operators were involved in the analysis. Agreement with the gold standard, defined as the mean of 2 manual measurements of a skilled operator, and the interobserver and intraobserver variability were quantitatively evaluated by regression analysis and Bland-Altman statistics. ***Results.*** The automatic measure of the CIMT showed a mean bias ± SD of 0.001 ± 0.035 mm toward the manual measurement. The intraobserver variability, evaluated with Bland-Altman plots, showed a bias that was not significantly different from 0, whereas the SD of the differences was greater in the manual analysis (0.038 mm) than in the automatic analysis (0.006 mm). For interobserver variability, the automatic measurement had a bias that was not significantly different from 0, with a satisfactory SD of the differences (0.01 mm), whereas in the manual measurement, a little bias was present (0.012 mm), and the SD of the differences was noticeably greater (0.044 mm). ***Conclusions.*** The CIMT has been accepted as a noninvasive marker of early vascular alteration. At present, the manual approach is largely used to estimate CIMT values. However, that method is highly operator dependent and time-consuming. For these reasons, we developed a new system for the CIMT measurement that conjugates precision with real-time analysis, thus providing considerable advantages in clinical practice. ***Key words:*** carotid artery; edge detection; intima-media thickness; real-time ultrasound imaging; thickness measurement.

Abbreviations
ANG, angle; AUTO, automatic; CI, confidence interval; CIMT, carotid intima-media thickness; COEFF, coefficient; FOAM, first-order absolute moment edge operator; GS, gold standard; GUI, graphical user interface; OP, operator; MAN, manual; MAX, maximum; PX, point; ROI, region of interest; TH, threshold

Received March 10, 2008, from the Institute of Clinical Physiology, National Research Council, Pisa, Italy (F.F., V.G., E.B., M.D.); Department of Internal Medicine, University of Pisa, Pisa, Italy (G.G., L.G.); and Esaote SpA, Genoa, Italy (M.D.). Revision requested March 31, 2008. Revised manuscript accepted for publication May 8, 2008.

This work was supported in part by Esaote SpA under grant IFC-Esaote-2006.

Address correspondence to Francesco Faita, PhD, Institute of Clinical Physiology, National Research Council, Via G. Moruzzi 1, 56124 Pisa, Italy.

E-mail: f.faita@ifc.cnr.it

An increased carotid intima-media thickness (CIMT) is a marker of early alterations of the arterial walls, which are associated with an increased risk of cardiovascular disease.[1] Assessment of this parameter can be performed with B-mode ultrasound imaging, a technique that is safe, relatively inexpensive, and suitable for large-scale population studies.[2] Thus, CIMT measurement is currently used as a surrogate cardiovascular end point in randomized controlled trials.[2,3] However, methods used for CIMT measurements in these trials have not been standardized, thus affecting the reproducibility and statistical power of the studies.[2]

The CIMT is defined as the distance between the leading edge of the lumen-intima interface and the leading edge of the media-adventitia interface. A manual approach is commonly used to locate such edges,[4] a method that is both highly operator dependent and time-consuming. Indeed, training and subjective judgment of the operator determine the variability of CIMT measurement, thus influencing the study results. This is a crucial issue because greater variability in the measurements requires a larger sample size to reach an appropriate statistical power in clinical studies. For these reasons, semiautomatic procedures using computer-assisted systems were introduced.[5–7] However, the major limitation of these first attempts was the considerable operator dependency, which can still cause large variability in the measurements. Other methods, based on the collection of raw radio frequency data,[8] were biased by the lack of availability of this kind of output data in commercial ultrasound systems, whereas automatic procedures based on multiscale dynamic programming still required some manual intervention after the automatic evaluation.[9] Computerized systems based on an active contour model,[10] analysis of the image gradient,[11] and an active contour technique improved by multiresolution analysis[12] were then introduced. These analyses were performed on stored images, and real-time implementation was not taken into account. However, real-time analysis can play an important role in the clinical practice for 2 main reasons: it is less time-consuming, and it offers visual feedback during the image acquisition. This second aspect is of particular importance because it can help the physician optimize the image quality, thus improving the robustness of the measurement.

In this report, we describe a real-time automatic technique for CIMT measurement based on a first-order absolute moment edge operator (FOAM), which is particularly robust against the speckle noise that characterizes echographic images, and a pattern recognition approach.

Materials and Methods

Study Population

The study population included 80 healthy participants (mean age ± SD, 35 ± 14 years; range, 18–55 years; 24 male) and 70 patients (mean age, 50 ± 7 years; range, 38–66 years; 42 male) with cardiovascular risk factors.

Inclusion criteria for patients were the presence of at least 1 of the following conditions: essential hypertension, dyslipidemia, an elevated fasting glucose level or diabetes, overweight or obesity, and smoking habits. A wide range of carotid arteries were analyzed to test the behavior of the algorithm with different images. The study protocol was approved by the local Ethics Committee, and informed consent was obtained from all volunteers.

Edge Operator

The edge detector we used is named FOAM. A more exhaustive description of the mathematical operator and its use in a generic task of edge detection can be found elsewhere.[13] In this report, we review just some of its characteristics, which are useful for describing the algorithm we developed for assessment of the CIMT.

Let $f(x,y)$ be the gray map of an image, and let Θ be a circular domain with area A_Θ whose center is the point with coordinates x,y; the following FOAM can be defined:

$$e(x,y) = \frac{1}{A_\Theta}\iint_\Theta \left| f(x,y) - f(x-\tau_x, y-\tau_y) \right| d\tau_x d\tau_y . \quad (1)$$

Equation 1 computes the mean dispersion of the values that $f(x,y)$ assumes at the points belonging to Θ with respect to the value that $f(x,y)$ assumes at the central points of Θ. When Equation 1 is computed at a point of discontinuity between the gray levels of an image, it gives rise to a local maximum.

However, in order to cope with different noise conditions, 2 low-pass filters and a weight function must be introduced:

$$e(x,y) = \iint \left| f_1(x,y) - f_2(x-\tau_x, y-\tau_y) \right| \cdot g(\tau_x, \tau_y, \sigma_3) d\tau_x d\tau_y \quad (2)$$

$$f_1(x,y) = f(x,y) \otimes g(x,y,\sigma_1)$$

$$f_2(x,y) = f(x,y) \otimes g(x,y,\sigma_2),$$

where $g(x,y,\sigma_i)$ are normalized gaussian functions.

Substantially, Equation 2 provides a ridge map similar to the map that is provided by the magnitude of a gradient of gaussian filter. However, unlike the gradient of gaussian magnitude, the FOAM exhibits a better signal-to-noise ratio when used in the presence of speckle noise.[14] In particular, the signal-to-noise ratio is substantially improved when small apertures σ_i are used, and in our application, small σ_i must be chosen to accurately locate the interfaces we are looking for. In this study, values of σ_i were chosen in agreement with the calibration factor, expressed as millimeters per pixel (Table 1). According to these properties, the use of the FOAM as an edge detector with ultrasound images is a preferable choice compared to the use of other most popular edge detectors.

Algorithm

Figure 1 shows a typical B-mode ultrasound image of the carotid artery and a schematic illustration of the edges and interfaces in the echo signal. Meaning edges can be mapped on the following interfaces: near wall media-adventitia, far wall lumen-intima, and far wall media-adventitia.

On ultrasound images, blood (vessel lumen) and wall layers have different echogenicity because of their differences in scatterer size and the number of scatterers per unit volume. The vessel lumen and tunica media do not appear to reflect ultrasound waves, thus allowing good identification of the lumen-intima and media-adventitia interfaces.

The longitudinal section axis of the carotid artery appears parallel to the horizontal axis in our coordinate system. The probe is placed on the external surface of the neck of the patient; thus, the orientation depends only on the position of the artery relating to the longitudinal axis of the neck. Because the common carotid artery can be considered parallel to this axis, one can then search for edges inside a region of interest (ROI) by proceeding along the vertical axis. Because the CIMT measure is defined as the distance between the lumen-intima and media-adventitia interfaces, the value of the CIMT can be evaluated when the position of these interfaces is known. The presence of artifacts in the images due to speckling, reverberations, and acoustic shadowing may turn the precise location of these interfaces into quite a challenging task.

For every frame of the video sequence, the image-processing scheme can be divided into 4 steps: (1) image filtering with the FOAM operator; (2) a heuristic search of local maxima; (3) removal of outliers with an iterative algorithm; and (4) CIMT evaluation.

Filtering Process

Given an echographic image of a longitudinal section of a carotid artery, Figure 2A shows the typical profile of the gray levels of a vertical column in the ROI when the latter includes the far wall of the artery only. Furthermore, Figure 2B

Table 1. Algorithm Parameters

Name	Value
σ_2	0.1417 mm/Calib
$\sigma_{1,3}$	$\sigma_2/2$
COEFF_1	0.4
COEFF_2	0.9
TH_PX_1	3 pixels
TH_PX_2	5 pixels
TH_ANG_1	5°
TH_ANG_2	3°

Calib indicates calibration factor, expressed as millimeters per pixel.

Figure 1. B-mode sonogram of the carotid artery with highlighted meaning interfaces.

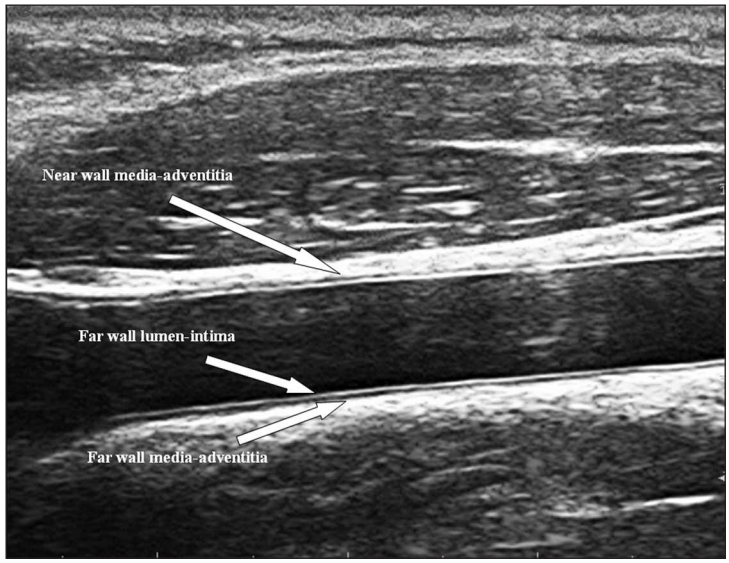

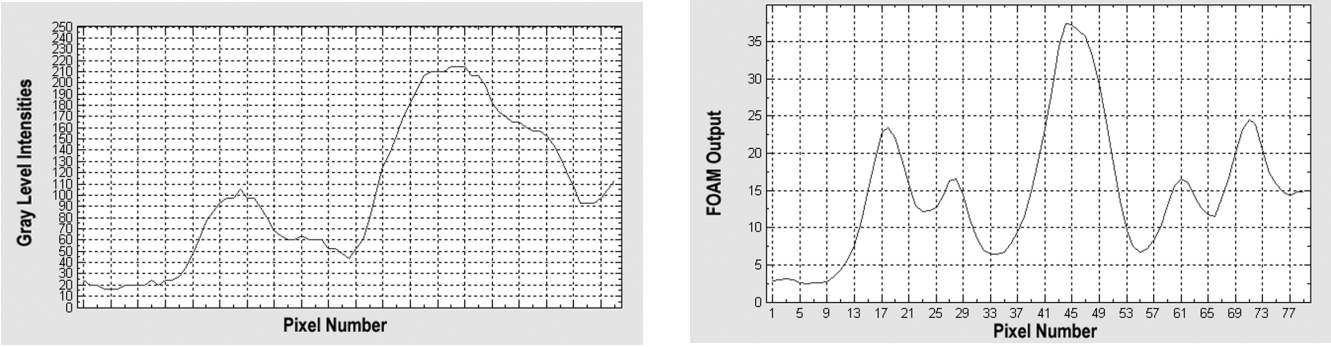

A B

Figure 2. A, Typical profile of the gray levels of a column of the ROI (near the far wall of the carotid artery). **B**, Profile of the column of the gray level represented in a after the filtering process with the FOAM operator.

shows the profile of the respective column of the gray level map, which is obtained by filtering the ROI with the FOAM operator. Points that are internal to the vessel are typically anechoic, whereas the tunica intima and tunica adventitia are the most reflective layers. That is, the FOAM response to points inside the lumen is very poor, and when moving from the latter toward the far wall, the lumen-intima and media-adventitia interfaces correspond to the first and third local maxima, left to right, respectively. The second local maximum, which is shown in Figure 2B, corresponds to the intima-media interface.

However, it is worth noting that real clinical images are not noiseless, and as a consequence, interfaces are not always well defined. Blood turbulences within the vessel, for example, can give rise to gray level discontinuities, which are very similar to those generated by the interfaces between the artery tunics. Consequently, reduced reliability in locating the carotid interfaces accurately is a drawback. We will show that a heuristic search for local maxima combined with a thresholding process can overcome this problem.

Heuristic Search

A heuristic search is applied to every column of the ROI. Let $FOAM\_MAX_i$ be the absolute maximum of the FOAM in the ith column of the ROI. For every single column of the ROI, the search algorithm performs the following 4 steps: (1) all local maxima are found and highlighted with a mark; (2) starting from the center of the lumen, the first maximum that is greater or equal to a first threshold (TH_1) is searched for, where TH_1 is obtained by multiplying $FOAM\_MAX_i$ by a coefficient (COEFF_1); (3) the second maximum following the first that is greater or equal to a second threshold (TH_2) is searched for, where TH_2 is obtained by multiplying the first maximum by a coefficient (COEFF_2); the second maximum often corresponds to the absolute maximum; and (4) if both maxima are found, the column is marked as "good"; otherwise it is marked as "bad."

The search algorithm is based on the following considerations: (1) the FOAM operator usually provides high local maxima at the lumen-intima and media-adventitia interfaces; (2) the FOAM response associated with blood turbulences and other artifacts is weaker than the response provided at the searched-for interfaces; and (3) the intima-media interface gives rise to a response of the FOAM operator that is weaker than the responses associated with the lumen-intima and media-adventitia interfaces, and according to this property, we are able to discard the local maxima associated with the intima-media interface. At the end of this stage, columns labeled good are selected. All the found points, however, must be now analyzed together to cope with noise and outliers.

Outlier Removal

This step is necessary to integrate all of the information previously stored and to exploit the constraint of continuity of the searched-for interfaces (ie, points of adjacent columns that belong to the same interface must be close to each other). Consequently, isolated points (outliers) are removed.

Moreover, because of the small vessel window under examination, the searched-for interfaces can be approximated as straight segments. Thus, on every interface, we can proceed as follows: (1) the least square regression line that best fits the points is computed; (2) points that are farther from the line than a threshold (TH_PX_1) are discarded; (3) a new least square regression line that best fits the points that have not been discarded is computed; and (4) the procedure is iterated until the last outlier has been removed. At the end of this stage, 2 regression lines are available, one for the lumen-intima interface and the other for the media-adventitia interface.

Carotid Intima-Media Thickness Evaluation

Three more controls are now necessary before the CIMT evaluation can be concluded. If one of these controls fails, the frame will be discarded. First, a minimum number of valid points (TH_PX_2) must remain to identify every interface after the outlier removal phase. Second, the slopes of the 2 regression lines cannot differ more than a given angle (TH_ANG_1). Third, the slope of each of the 2 regression lines cannot differ more than a given value (TH_ANG_2) from the mean value of the slope evaluated in the 5 previous frames. If the frame has not been discarded, the CIMT is evaluated as the distance between the mean point of the first regression line (lumen-intima interface) and the second regression line (media-adventitia interface).

Video-Processing System

The algorithm is implemented on a stand-alone video-processing device based on a digital signal-processing board. The main component is the Texas Instruments TMS320C6415 (Texas Instruments Incorporated, Dallas, TX), a high-performance digital signal processor particularly suited for computationally intensive video-processing applications. The device acquires the analog video signal from an ultrasound system and shows the results on a graphical user interface (GUI; Figure 3). A mouse and a keyboard are available to operate the device. The interaction of the sonographer with the system is reduced to the preliminary calibration phase and to the choice of the ROI where only the lumen-intima and media-adventitia interfaces are present. The procedure starts once the sonographer has correctly positioned the ultrasound probe on the neck of the patient and has traced the ROI on the GUI window, where the ultrasound images are displayed in real time. After this simple initialization procedure, the elaboration starts. The value of the CIMT is shown by a numeric display. Once initialized, the system does not require any intervention by the sonographer, who will direct efforts toward obtaining a good-quality image. When the quality of the measurement is judged good by the clinical operator, the value can be stored in memory by simply pressing a button on the GUI. More information on the hardware and software architecture of the equipment can be found in our previous work.[15]

Experimental Protocol

In vivo images were used to validate the system: 150 images from 150 participants were analyzed, both with manual measurements and with the presented automatic method.

Carotid ultrasound images were obtained by high-resolution B-mode ultrasound with a 7.5- to 12-MHz linear array transducer (MyLab25; Esaote SpA, Genoa, Italy). The left and right common carotid arteries were examined in

Figure 3. Graphical user interface of the application for CIMT assessment.

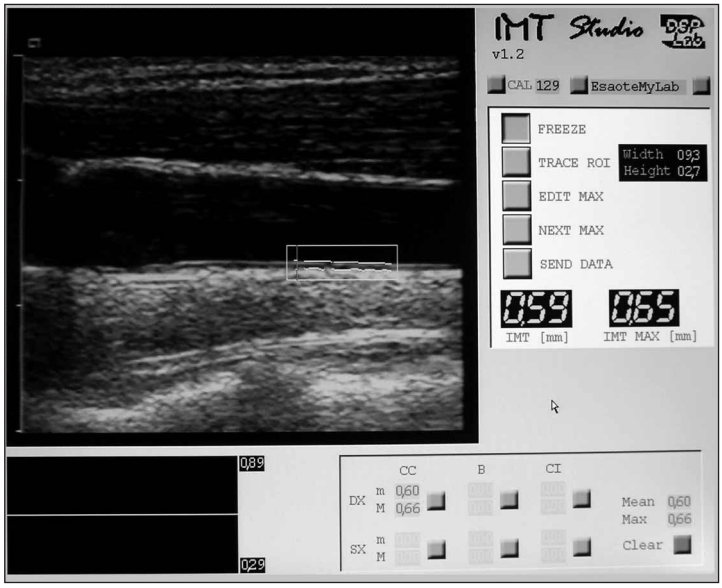

anterolateral, posterolateral, and mediolateral directions. Longitudinal images of the distal common carotid arteries were obtained. The CIMT was measured in the far wall of the common carotid artery 1 cm proximal to the carotid bulb in a region free of plaques. Images from healthy participants and patients were acquired by a certified sonographer specially trained in CIMT measurement.

Two skilled operators were involved in the analysis. The first operator (OP1) performed 2 manual and 2 automatic measurements on every image. The second operator (OP2) performed 1 manual and 1 automatic measurement. The gold standard (GS) measurement was defined as the mean of OP1's 2 manual measurements.

For validation purposes, we developed a MATLAB (The MathWorks, Natick, MA) GUI to manually trace the contours because calipers of the ultrasound equipment are unreliable for this aim and do not allow tracing of splines. With this software, all manual measurements were obtained. Physicians were allowed to place several points to locate the intima-media and media-adventitia interfaces on every frame. From these points, 2 segments were interpolated, and the distance between them was considered the CIMT value for the corresponding frame.

Statistical Analysis

Agreement with the GS and the interobserver and intraobserver variability were quantitatively evaluated by means of regression analysis and Bland-Altman statistics. The robustness, ie, the capability of providing results without apparent failures, was estimated by the number of frames where the algorithm was able to find the searched-for interfaces with respect to the total image number.

Results

The algorithm parameters are summarized in Table 1. The mean value, SD, and range of the CIMT measurements obtained by different operators and trials are shown in Table 2. The agreement and interobserver and intraobserver variability between the automatic (AUTO) system and manual (MAN) method are shown in Figures 4–8 and Tables 3–5.

Figure 4 shows a Bland-Altman plot that compares automatic and GS measurements performed by OP1. Table 3 reports the results of the comparison. The measure of the CIMT had a bias of 0.001 mm, and the SD of the differences was 0.035 mm.

The intraobserver variability was evaluated by Bland-Altman plots, which compared OP1's 2 manual and 2 automatic measurements (Figures 5 and 6). In both cases, the bias was not significantly different from 0, whereas the SD of the differences was greater in the manual analysis (0.038 mm) than in the automatic analysis (0.006 mm).

The interobserver variability was evaluated by Bland-Altman plots, which compared the manual and automatic measurements of the first operator against the second (Figure 7 and 8). In the automatic case, the bias was not significantly different from 0 with, moreover, a satisfactory SD of the differences for this kind of measurement (0.01 mm). On the contrary, in the manual case a little bias was present (0.012 mm), and the SD of the differences was noticeably greater (0.044 mm) than in the automatic analysis. Tables 4 and 5, summarize the results of the interobserver and intraobserver analysis, respectively. For robustness, the proposed algorithm failed to find the lumen-intima and media-adventitita interfaces in 3 of the 150 analyzed frames.

Table 2. Mean Value, SD, and Range of the CIMT Measurements From Both Healthy Participants and Patients Obtained by Different Operators and Trials

Trial	Mean, mm	SD, mm	Range, mm
OP1, trial 1, MAN	0.56	0.14	0.35–1.15
OP1, trial 2, MAN	0.57	0.14	0.36–1.12
OP1, trial 1, AUTO	0.57	0.14	0.35–1.05
OP1, trial 2, AUTO	0.57	0.14	0.35–1.05
OP2, MAN	0.56	0.14	0.31–1.13
OP2, AUTO	0.57	0.14	0.35–1.05

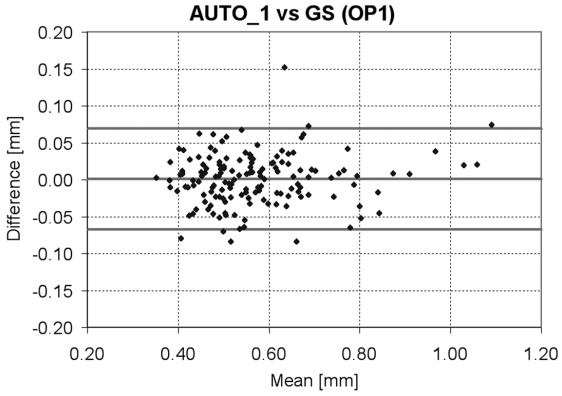

Figure 4. Comparison with respect to the GS measure: Bland-Altman plot.

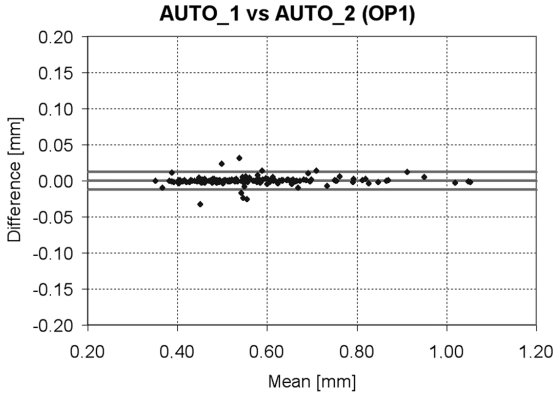

Figure 6. Comparison between automatic measurements of OP1: Bland-Altman plot.

Discussion

The carotid CIMT has been accepted as a noninvasive marker of early vascular alterations, including atherosclerosis and vascular remodeling.[1] Thus, it is widely used in clinical practice.

Normal CIMT values range from 40 to 80 µm in healthy individuals, whereas values of greater than 90 µm identify subclinical vascular damage in special populations, such as hypertensive patients.[16] For this reason, great sensitivity in the measurement is needed.

At present, the manual approach is largely used to estimate CIMT values in clinical studies and practice.[17] However, this method has several shortcomings. In particular, it is highly subjective to the skills of the operator because the highlighting of the intima-media and media-adventitia layers is strictly connected to the visual perception of the echographic interfaces. Moreover, manual measurements are time-consuming.

The method reported here shows good agreement with the GS and can be considered a valid alternative to the manual measurements. Of importance, although the manual method showed variability similar to those reported in the literature,[17] the proposed method showed less interobserver and intraobserver variability than that associated with the manual method. Consequently, population studies, multicenter research, and follow-up studies would be characterized by greater statistical significance when based on the automatic method.

Figure 5. Comparison between manual measurements of OP1: Bland-Altman plot.

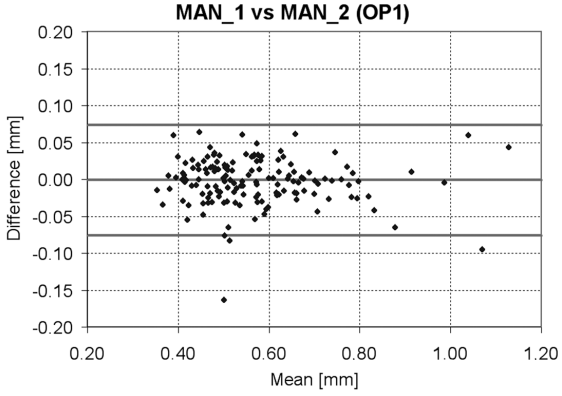

Figure 7. Comparison between manual measurements of OP1 and OP2: Bland-Altman plot.

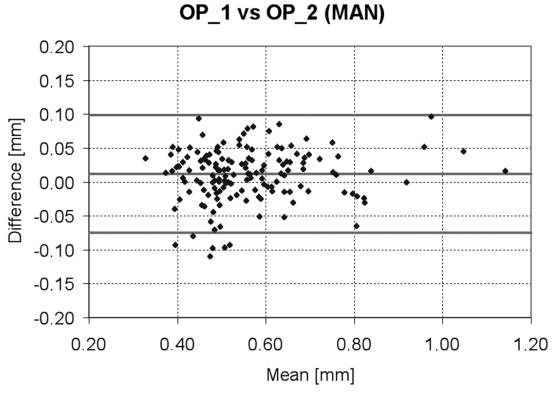

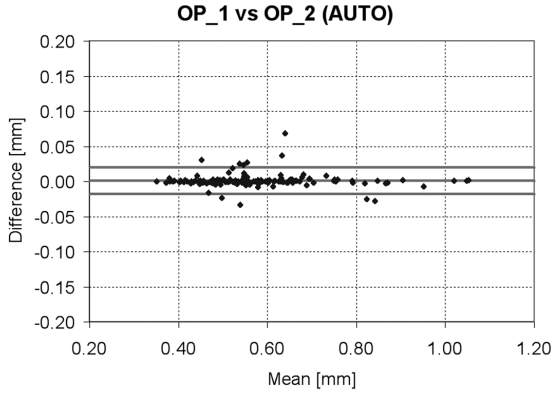

Figure 8. Comparison between automatic measurements of the OP1 and OP2: Bland-Altman plot.

Table 3. Comparison With Respect to the GS Measure: Results of the Bland-Altman Analysis

Parameter	AUTO_1 vs GS (OP1), mm
Bias	0.001
SD	0.035
Interval of agreement	±0.068
95% CI for bias	0.006
95% CI for limits of agreement	0.01

CI indicates confidence interval.

Table 4. Intraobserver Variability: Results of the Bland-Altman Analysis

Parameter	MAN_1 vs MAN_2 (OP1), mm	AUTO_1 vs AUTO _2 (OP1), mm
Bias	–0.001	0
SD	0.038	0.006
Interval of agreement	±0.075	±0.012
95% CI for bias	0.006	0.001
95% CI for limits of agreement	0.011	0.002

Table 5. Interobserver Variability: Results of the Bland-Altman Analysis

Parameter	OP1 vs OP2 (MAN), mm	OP1 vs OP2 (AUTO), mm
Bias	0.012	0.001
SD	0.044	0.01
Interval of agreement	±0.087	±0.019
95% CI for bias	0.007	0.002
95% CI for limits of agreement	0.012	0.003

Other automatic methods have been reported in the literature. Liang et al[9] developed an automatic procedure based on multiscale dynamic programming to automatically measure the CIMT on ultrasound images. As the authors acknowledged, such a procedure requires some manual intervention after the automatic evaluation, and the system must be adapted when the ultrasound equipment changes. Schmidt-Trucksäss et al[10] introduced a computerized system based on an active contour model; Liguori et al[11] developed a system based on analysis of the image gradient; and Gutierrez et al[12] introduced an active contour technique, which was improved by multiresolution analysis. These last 3 methods, however, did not address the issue of real-time implementation, which has an important role in clinical practice.

The real-time capabilities of the system we have described are particularly useful for assisting physicians in adjusting image quality when measurement is still in progress. Moreover, with real-time analysis, evaluation of the CIMT can be easily available not only on a single frame but also during the whole cardiac cycle, thus obtaining a more robust assessment. Additionally, the implemented algorithm is based on an edge operator (FOAM), which has a better signal-to-noise ratio in the presence of speckle noise with respect to traditional edge detectors such as laplacian of gaussian and gradient of gaussian, thus ensuring great precision in the CIMT assessment. Finally, the system is not constrained to a specific apparatus because it requires only a simple analog video signal, which is usually provided by all commercial echographic equipment.

In conclusion, the described system conjugates precision with real-time analysis, and this might provide considerable advantages for CIMT assessment in clinical practice.

References

1. Lorenz MW, Markus HS, Bots ML, Rosvall M, Sitzer M. Prediction of clinical cardiovascular events with carotid intima-media thickness: a systematic review and meta-analysis. Circulation 2007; 115:459–467.

2. Bots ML, Evans GW, Riley WA, Grobbee DE. Carotid intima-media thickness measurements in intervention studies: design options, progression rates, and sample size considerations—a point of view. Stroke 2003; 34:2985–2994.

3. Wang JG, Staessen JA, Li Y, et al. Carotid intima-media thickness and antihypertensive treatment: a meta-analysis of randomized controlled trials. Stroke 2006; 37:1933–1940.

4. Howard G, Sharrett AR, Heiss G, et al. Carotid artery intimal-media thickness distribution in general populations as evaluated by B-mode ultrasound. ARIC Investigators. Stroke 1993; 24:1297–1304.

5. Touboul PJ, Prati P, Scarabin PY, Adrai V, Thibout E, Ducimetière. Use of monitoring software to improve the measurement of carotid wall thickness by B-mode imaging. J Hypertens Suppl 1992; 10:S37–S41.

6. Gariepy J, Massonneau M, Levenson J, Heudes D, Simon A. Evidence for in vivo carotid and femoral wall thickening in human hypertension. Groupe de Prévention Cardio-vasculaire en Médecine du Travail. Hypertension 1993; 22: 111–118.

7. Selzer RH, Hodis HN, Kwong-Fu H, et al. Evaluation of computerized edge tracking for quantifying intima-media thickness of the common carotid artery from B-mode ultrasound images. Atherosclerosis 1994; 111:1–11.

8. Hoeks AP, Willekes C, Boutouyrie P, Brands PJ, Willigers JM, Reneman RS. Automated detection of local artery wall thickness based on M-line signal processing. Ultrasound Med Biol 1997; 23:1017–1023.

9. Liang Q, Wendelhag I, Wikstrand J, Gustavsson T. A multiscale dynamic programming procedure for boundary detection in ultrasonic artery images. IEEE Trans Med Imaging 2000; 19:127–142.

10. Schmidt-Trucksäss A, Cheng DC, Sandrock M, et al. Computerized analysing system using the active contour in ultrasound measurement of carotid artery intima-media thickness. Clin Physiol 2001; 21:561–569.

11. Liguori C, Paolillo A, Pietrosanto A. An automatic measurement system for the evaluation of carotid intima-media thickness. IEEE Trans Instrum Meas 2001; 50: 1684–1691.

12. Gutierrez MA, Pilon PE, Lage SG, Kopel L, Carvalho RT, Furuie SS. Automatic measurement of carotid diameter and wall thickness in ultrasound images. In: Proceedings of the 29th Annual Conference of Computers in Cardiology. Piscataway, NJ: Institute of Electrical and Electronics Engineers; 2002:359–362.

13. Demi M, Paterni M, Benassi A. The first absolute central moment in low-level image processing. Comput Vis Image Underst 2000; 80:57–87.

14. Faita F, Gemignani V, Giannoni M, Benassi A, Demi M. The first-order absolute moment as an edge-detector in cardiovascular imaging: a comparison with two well-known edge-detectors. In: Proceedings of the 31th Annual Conference of Computers in Cardiology. Piscataway, NJ: Institute of Electrical and Electronics Engineers; 2004: 561–564.

15. Gemignani V, Faita F, Giannoni M, Benassi A. A DSP-based platform for rapid prototyping of real time image processing systems. In: Proceedings of the Third Internation Symposium on Image Signal Processing and Analysis. Vol 2. Piscataway, NJ: Institute of Electrical and Electronics Engineers; 2003:936–939.

16. Mancia G, De Backer G, Dominiczak A, et al. 2007 ESH-ESC Practice Guidelines for the Management of Arterial Hypertension: ESH-ESC Task Force on the Management of Arterial Hypertension. J Hypertens 2007; 25:1751–1762.

17. Simon A, Gariepy J, Chironi G, Megnien JL, Levenson J. Intima-media thickness: a new tool for diagnosis and treatment of cardiovascular risk. J Hypertens. 2002; 20:159–169.